Hedgehog signalling pathway orchestrates angiogenesis in triple-negative breast cancers

Concetta Di Mauro[1], Roberta Rosa[1], Valentina D'Amato[1], Paola Ciciola[1], Alberto Servetto[1], Roberta Marciano[1], Roberta Clara Orsini[1], Luigi Formisano[1], Sandro De Falco[2], Valeria Cicatiello[2], Maurizio Di Bonito[3], Monica Cantile[3], Francesca Collina[3], Angela Chambery[4], Bianca Maria Veneziani[5], Sabino De Placido[1] and Roberto Bianco*,[1]

[1]Department of Clinical Medicine and Surgery, University of Naples 'Federico II', Naples, Italy; [2]Angiogenesis Laboratory, Institute of Genetics and Biophysics, 'Adriano Buzzati-Traverso', Consiglio Nazionale delle Ricerche (CNR), Naples, Italy; [3]Division of Diagnostic Pathology, Department of Diagnostic and Laboratory Pathology, 'Istituto Nazionale Tumori Fondazione Giovanni Pascale–IRCCS', Via Mariano Semmola, Naples, Italy; [4]Department of Environmental, Biological and Pharmaceutical Sciences and Technologies, Second University of Naples, Naples, Italy and [5]Department of Molecular Medicine and Medical Biotechnologies, University of Naples 'Federico II', Naples, Italy

Background: Several evidences suggest a marked angiogenic dependency in triple-negative breast cancer (TNBC) tumorigenesis and a potential sensitivity to anti-angiogenic agents. Herein, the putative role of Hedgehog (Hh) pathway in regulating TNBC-dependent angiogenesis was investigated.

Methods: Expression and regulation of the Hh pathway transcription factor glioma-associated oncogene homolog1 protein (GLI1) were studied on the endothelial compartment and on TNBC-initiated angiogenesis. To evaluate the translational relevance of our findings, the combination of paclitaxel with the Smo inhibitor NVP-LDE225 was tested in TNBC xenografted mice.

Results: Tissue microarray analysis on 200 TNBC patients showed GLI1 overexpression paired with vascular endothelial growth factor receptor 2 (VEGFR2) expression. *In vitro*, Hh pathway promotes TNBC progression in an autocrine manner, regulating the VEGF/VEGFR2 loop on cancer cell surface, and in a paracrine manner, orchestrating tumour vascularisation. These effects were counteracted by Smo pharmacological inhibition. In TNBC xenografted mice, scheduling NVP-LDE225 rather than bevacizumab provided a better sustained inhibition of TNBC cells proliferation and endothelial cells organisation.

Conclusions: This study identifies the Hh pathway as one of the main regulators of tumour angiogenesis in TNBC, thus suggesting Hh inhibition as a potential new anti-angiogenic therapeutic option to be clinically investigated in GLI1 overexpressing TNBC patients.

Triple-negative breast cancer (TNBC) is an aggressive histological subtype characterised by lack of oestrogen receptor (ER), progesterone receptor (PgR) and human epidermal growth factor receptor 2 (HER2) expression. Accounting for 10–17% of all breast carcinomas (Haffty *et al*, 2006; Penault-Llorca and Viale, 2012), TNBC is more aggressive than other breast tumours; it is often correlated with shorter disease-free and overall survival (OS) compared with those of women affected by non-TNBC (Dent *et al*, 2007; Liedtke *et al*, 2008) Chemotherapy remains the main therapeutic option for TNBC patients, since neither endocrine therapies nor HER2-targeted agents are effective. Due to poor prognosis and restricted therapeutic chances (Chacón and Costanzo, 2010; Palma *et al*, 2015), new targeted therapies for TNBC are required to improve the outcome of this subset of breast cancer.

Published data have shown that TNBC tumours express high levels of intratumoural vascular endothelial growth factor (VEGF) (Linderholm *et al*, 2009), possess high microvessel density

Published by Springer Nature on behalf of Cancer Research UK.

1425

(Mohammed *et al*, 2011) and display VEGF gene amplification compared to non-TNBC tumours (André *et al*, 2009), suggesting a marked angiogenic dependency in TNBC tumorigenesis and a potential sensitivity to anti-angiogenic agents. In fact, the treatment with the anti-VEGF monoclonal antibody (mAb) bevacizumab has shown some benefit when combined with standard chemotherapy (Bear *et al*, 2012) albeit the therapeutic use of bevacizumab and its clinical relevance in TNBC treatment is in the centre of a controversy. As a matter of fact, several studies demonstrated an approximate doubling of progression-free survival compared with placebo despite no benefit in OS associated with the use of bevacizumab was obtained (Gray *et al*, 2009; Miles *et al*, 2010; Robert *et al*, 2011).

The Hedgehog (Hh) signalling pathway, playing a crucial role in cell proliferation and differentiation, also regulates angiogenesis and vascular formation in early embryonic development (Nagase *et al*, 2008; Pak and Segal, 2016). The binding of Hh ligands to Patched (PTCH), a 12 pass transmembrane protein, causes a release of its inhibitory action on Smoothened (Smo) (Rohatgi *et al*, 2009; Cohen, 2010); activated Smo initiates a signalling cascade leading to glioma-associated oncogene homolog 1 proteins (GLI1) activation, which induces the transcription of downstream target genes, thus regulating cellular cycle and apoptosis (Katoh and Katoh 2009; Shahi *et al*, 2010). An aberrant activation of the pathway, occurring in many tumours, has been described in breast cancer development and progression (O'Toole *et al*, 2011; Riku *et al*, 2016), where it regulates the promotion of epithelial–stromal interactions (Yauch *et al*, 2008; Theunissen and de Sauvage, 2009; Angelucci *et al*, 2012). Emerging data support Hh pathway contribution to cancer cell stemness in TNBC (Habib and O'Shaughnessy, 2016). Furthermore, the expression of some Hh effectors, such as Smo and GLI1, is significantly increased in TNBC in comparison to non-TNBC (Tao *et al*, 2011).

Several recent data suggest the involvement of Hh signalling in tumour-associated angiogenesis: the ligand sonic Hedgehog homolog (SHH) can promote angiogenesis in a paracrine manner, stimulating the production of secreted factors (Yamazaki *et al*, 2008). Glioma-associated oncogene homolog1 protein, the main transcription factor of the Hh pathway, leads to upregulation of a pro-angiogenic secreted molecule, cysteine-rich angiogenic inducer 61 (CYR61) (Harris *et al*, 2012) and of neuropilin 2 (NRP2), a VEGFR1 and vascular endothelial growth factor receptor 2 (VEGFR2) co-receptor (Goel *et al*, 2013). An alternative splicing form of GLI1, 4 kDa shorter than full length (truncated GLI1 or tGLI1), enhances the hVEGF-A gene promoter, leading to upregulation of this factor in breast cancer cells (Cao *et al*, 2012; Carpenter and Lo, 2012).

The purpose of this study was to evaluate the complexity of aberrant Hh pathway functions in TNBC and its putative effect in sustaining TNBC angiogenesis, suggesting the Hh pathway inhibition as a new anti-angiogenic therapeutic option in this subtype of tumour.

MATERIALS AND METHODS

Compounds and cell cultures. NVP-LDE225 and paclitaxel were purchased from Selleck Chemicals (Munich, Germany). Bevacizumab was kindly provided by Roche (Basel, Switzerland).

For this study, a panel of immortalised (MDA-MB-361, SKBR-3, MCF7, MDA-MB-231, HCC70 and MDA-MB-468, KPL-4, JIMT-1) and primary (K90, K79, K193 and K197) breast cancer cell lines were used. Besides, some experiments have been performed on endothelial cells such as human umbilical vein endothelial cells (HUVECs) and mouse brain endothelial cell 5 (bEND5). For a detailed description, please see the Supplementary Methods section.

Western blot analysis. Total protein extracts obtained from cell cultures or tumour specimens were resolved by 4–15% SDS–PAGE and probed with anti-human GLI11, Smo, VEGFR2, NRP2, pAkt/Akt, pERK/ERK, cyclin D1, bcl2 and GAPDH (Cell Signaling Technologies, Beverly, MA, USA). Immunoreactive proteins were visualised by enhanced chemiluminescence (Pierce, Rockford, IL, USA).

Capillary tube formation assay. Twenty-four-well plates were coated with 200 μl per well of Matrigel (BD Biosciences, Billerica, MA, USA), allowed to jellify for 30 min at 37 °C in a cell culture incubator; HUVEC cells (5×10^4 per well) were plated on top of the Matrigel in TNBC or nTNBC-conditioned growth media, or in RPMI medium supplemented with VEGF-A (100 ng ml^{-1}), as a positive control. Cells were observed under an inverted microscope Olympus CKX31 (Olympus, Shinjuku, Tokyo, Japan) at regular intervals, and pictures were taken after 3 h.

Co-culture of tumour and endothelial cells. The *in vitro* co-culture model was prepared on Transwell polycarbonate filters (surface area, 0.3 cm^2; pore size, 0.3 μm; BD Biosciences, Franklin Lakes, NJ, USA). Brain endothelial cells 5 (2×10^4 per well) were seeded on the bottom of wells in a 24-multiwell plate, were allowed to adhere for 24 h, then TNBC or nTNBC cells (5×10^3 per well) were seeded on filters. Tumour and endothelial cells were cultured together for 3 days in DMEM medium.

The percentage of cell density was determined using the 3-(4,5-dimethylthiazol-2-yl)-2,5-diphenyltetrazolium bromide (MTT) assay according to the manufacturer's instructions (Sigma-Aldrich, Milan, Italy).

ELISA assay for the determination of VEGF-A, sVEGFR2 and THBS1 concentrations. Anti-human VEGF polyclonal antibody (R&D Systems, Minneapolis, MN, USA), diluted at 1 μg ml^{-1} in PBS pH 7.5, was used to coat a 96-well plate, 100 μl per well, overnight at 4 °C. Washings, dilutions of standards (recombinant hVEGF) and samples (conditioned media (CM) from tumour cells or sera from killed mice), biotinylation and mixtures with preformed avidin and biotinylated HRP macromolecular complex (Vectastain kit) were performed as previously described (D'Amato *et al*, 2014). Absorbance was measured at 490 nm on a microplate reader (Bio-Rad, Hercules, CA, USA). VEGF concentrations were determined by interpolation of the standard curve using linear regression analysis.

Soluble VEGFR2 (sVEGFR2) and thrombospondin1 (THBS1) concentrations on CM from tumour cells or sera from killed mice have been measured by using sVEGFR2 and THBS1 Quantikine ELISA kits (R&D Systems).

Multiplexed immunoassay. The quantitative analysis of secreted cytokines and chemokines in CM of MDA-MB-231, SUM-159, SUM-149, HCC70 and MDA-MB-468 in the presence or absence of NVP-LDE225 (2.5 μM), was performed by the Bio-Plex multiplex system (Bio-Rad, Milan, Italy), based on xMAP technology that uses magnetic beads coated with specific antibodies raised against target analytes. For a detailed description, please see the Supplementary Methods section.

RNA extraction and analysis. Total RNA was isolated from cells using TRIZOL reagent (Invitrogen, Carlsbad, CA, USA). About 2 μg of total RNA was reverse transcribed using 100 ng of random hexamer primers and Super Script III Reverse Transcriptase (Invitrogen). Real-time RT–PCR (qRT-PCR) experiments were performed using the CFx96 Real-Time PCR Detection System (Bio-Rad); PCR reactions were in a final volume of 15 μl, using 5 ng of cDNA and iQ SYBR Green Supermix 2X (Bio-Rad). Reagents and enzymes were employed according to manufacturer's instructions. PCR cycling profile consisted of a cycle at 95 °C for 10 min and 40 two-step cycles at 95 °C for 10 s and at 60 °C for 60 s.

Primers were chosen using Primer3 software (http://bioinfo.ut.ee/primer3/) and designed to span exon/exon borders; their sequences are listed in the Supplementary Table S1. Three different RNA preparations were tested for each sample, and each reaction was run in triplicate.

RNA interference. Smart siRNA pool against all isoforms of GLI1 was purchased from Dharmacon (GE Dharmacon, Lafayette, CO, USA). A non-sense sequence was used as a negative control. For siRNA validation, cells were transfected with GLI1 siRNAs ($50 \, nmol \, l^{-1}$) using DharmaFECT 1 Transfection Reagent in DMEM (GE Dharmacon); 24 and 48 h after transfection, western blot analysis for GLI1 and VEGFR2 expression was performed.

Cell transfection with GLI1 expression vectors. MDA-MB-231 cells were cultured in RPMI medium supplemented with 10% FBS, $100 \, U \, ml^{-1}$ penicillin and $100 \, \mu g \, ml^{-1}$ streptomycin (all from Invitrogen) and grown at $37 \, ^{\circ}C$ in a humidified atmosphere containing 5% CO_2. For transfection, $5 \, \mu g$ of either pCMV6-GFP GLI1, pCMV6-GFP tGLI1, pCMV6-GFP empty vector plasmid (Origene, Rockville, MD, USA) were added together with lipofectamine 2000 Reagent (Invitrogen), following the manufacturer's instructions.

Luciferase assay. Luciferase assay was performed by using the Dual-Luciferase Assay system (Promega, Madison, WI, USA) following the manufacturer's protocol. A total of 5×10^5 MDA-MB-468 cells were plated 24 h before transfection in a 24-well multiwell plate. The GLI-Luc reporter plasmid (Promega) was transfected together with pRL-TK, encoding the Renilla luciferase (Promega), in triplicate, using lipofectamine 2000 Reagent (Invitrogen) with the luciferase reporter. Twenty-four hours after transfection, cells were treated with NVP-LDE225 $5 \, \mu M$. Luciferase activity was determined 48 h after transfection by using a BioTek Microplate Luminescence Reader (BioTek, Winooski, VT, USA).

ChIP assay. The chromatin immunoprecipitation (ChIP) assay was performed in MDA-MB-468 cells using ChIP Assay Kit (Millipore, Billerica, MA, USA) following the manufacturer's instructions. Crosslinking of the target proteins to the chromatin DNA with formaldehyde and breaking of the chromatin DNA into fragments (200–1200 bp) were performed. Immunoprecipitation (IP) of the protein–DNA complex was performed using a GLI1 antibody (Santa Cruz Biotechnology, Heidelberg, Germany). The DNA in IP products was amplified by RT–PCR with ChIP assay primers specific for the VEGFR2 promoter (500 nucleotides before start codon site). Primers sequences are listed in the Supplementary Table S2. Results were reported as fold changes relative to input.

Orthotopic breast xenograft model in nude mice. Five-week-old Balb/cAnNCrlBR athymic (nu+/nu+) mice (Charles River Laboratories, Milan, Italy) maintained in accordance with institutional guidelines of the University of Naples Animal Care Committee and in accordance with the Declaration of Helsinki were injected into the fourth mammary fat pad with MDA-MB-468 cells (10^7 cells per mice) resuspended in $200 \, \mu l$ of Matrigel (BD Biosciences). Seven days after the tumour cell injection, tumour-bearing mice were randomly assigned ($n = 10$ per group) to receive the following: NVP-LDE225 $20 \, mg \, kg^{-1}$ *per os* every day for 4 weeks; bevacizumab $5 \, mg \, kg^{-1}$ intravenously (i.v.), twice a week for 4 weeks, or a combination of these agents with paclitaxel i.v. $10 \, mg \, kg^{-1}$ once a week for 4 weeks. Tumour diameter was assessed with a vernier caliper, and tumour volume (cm^3) was measured using the formula $\pi/6 \times$ (larger diameter) $\times$ (smaller diameter)^2. Mice were killed when the tumour reached a volume of $2 \, cm^3$, the maximum size allowed by the Ethics Committee.

TMA building. A breast tissue micro array (TMA) was constructed using 237 samples of TNBC collected from 2003 to 2013 from the Pathology Unit of the Istituto Nazionale Tumori of Naples. Informed consent was obtained from all patients. All

tumours and controls were reviewed by two experienced pathologists (MDB/MC) according to the WHO classification criteria, using standard tissue sections and appropriate immuno-histochemical slides. Discrepancies between two pathologists from the same case were resolved in a joint analysis of the cases. Moreover, all specimens were characterised for all routinely diagnostic immunophenotypic parameters (ER, PGR, HER2 and Ki67). Tissue micro array was built using the most representative areas from each single case with one replicate. Tissue cylinders with a diameter of 1 mm were punched from morphologically representative tissue areas of each 'donor' tissue block and brought into one recipient paraffin block ($3 \times 2.5 \, cm$) using a semi-automated tissue arrayer (Galileo TMA).

Immunohistochemical analysis. For immunoistochemical analysis on mice tumour specimens, excised tumours were split into two halves and immediately fixed in 10% buffered formalin solution. Twelve hours later, tissues were embedded in paraffin in an automated tissue processor. Sections ($4–5 \, \mu m$) were then cut with a serial microtome and mounted on adhesive poly-L-lysine-coated slides. After being dried in an oven at $40 \, ^{\circ}C$ for 8 h, the slides were processed for immunohistochemistry (IHC) in a semi-automated machine (Menarini Bond Max, Menarini, Florence, Italy) with the following antibodies: CD31, GLI1, NRP2 and VEGFR2 (Novocastra, Newcastle, UK).

Immunohistochemical staining on TMA slides was done from formalin-fixed, paraffin-embedded tissues to evaluate the expression of GLI1 and VEGFR2 markers in human tumours. There are not standardised criteria for VEGFR2 and Gli1 markers staining evaluation. The staining intensity was graded as follows: 0, negative; 1, weak; 2, moderate; and 3, intense; the proportion was graded according to the percentage of positive cells as follows: 0, negative; 1, 1–14%; 2, $\geqslant$15%. The intensity score and proportion score were multiplied in order to generate an immunoreactive score (IS). An IS 0 defines negative expression, IS ranging between 1 and 3 defines moderate expression and IS >3 high expression. For a detailed description, please see the Supplementary Methods section.

For further details concerning the Materials and Methods used in this work, please see the Supplementary Methods section.

RESULTS

GLI1 expression correlates with VEGFR2 in TNBC patients. To evaluate the relevance of Hh pathway activation in TNBC, we analysed a TNBC TMA by IHC. The patient cohort included 237 TNBC samples of breast cancers; the age of patients ranged from 24 to 93 years (average age = 57 years). Clinicalpathological characteristics and follow-up data of TNBC patients are depicted in Supplementary Table S3. Excluding the samples that could not be assessed for the expression of both VEGFR2 and GLI1, the evaluable cases were 200 out of 237. For each marker, tumour samples were classified based on the IS (see Materials and Methods section). As shown in Figure 1A, 9 out of 200 TNBC samples (4.5%) showed high expression for VEGFR2 (IS >3), 20 out of 200 (10.0%) showed moderate expression (1 $<$ IS $<$ 3), while 171 out of 200 cases (85.5%) resulted negative (IS $=0$). In 24 out of 200 cases (12.0%), there was a high GLI1 expression (IS >3), in 53 out of 200 cases (26.5%) there was a moderate expression (1 $<$ IS $<$ 3) and in 123 out of 200 cases (61.5%) there was no GLI1 expression with IS $=0$ (Figure 1B). Considering the 20 samples with VEGFR2 IS ranging from 1 to 3, 7 out of 20 cases (35.0%) were negative for GLI1 expression (IS $=0$), 9 out of 20 (45.0%) showed moderate expression for GLI1 (1 $<$ IS $<$ 3) and 4 out of 20 (20.0%) showed GLI1 high expression (IS >3). Notably, among the 9 samples
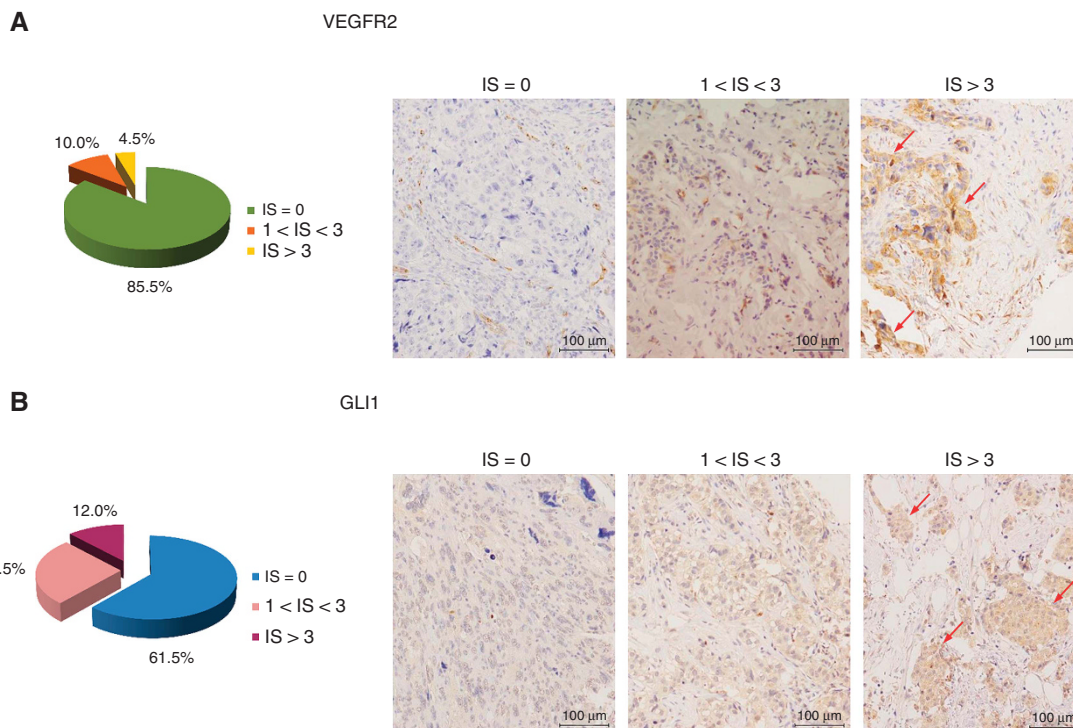
Figure 1. GLI1 expression correlates with VEGFR2 in TNBC patients. (**A**) Left, pie chart representing the percentage of samples included in the TMA that show immunoreactive score (IS) equal to 0, $1<IS<3$ and $IS>3$ for VEGFR2 expression. Right, immunoistochemical images representing VEGFR2 negative ($IS=0$) or -positive tumours with moderate ($1<IS<3$) and high ($IS>3$) expression levels, respectively. Endothelial cells positivity represents internal control ($\times 20$ magnification). The red arrows indicate representative highly VEGFR2 positive signal. (**B**) Left, pie chart representing the percentage of samples included in the TMA that show IS equal to 0, $1<IS<3$ and $IS>3$ for GLI1 expression, respectively. Right, immunoistochemical images representing GLI1-negative ($IS=0$) or -positive tumours with moderate ($1<IS<3$) or high ($IS>3$) expression levels, respectively ($\times 20$ magnification). The red arrows indicate representative highly GLI1 positive signal.

Table 1. Correlation between GLI1 and VEGFR2 expression in TNBC patients

	GLI1			P-value	R Pearson
	IS = 0	**1 < IS < 3**	**IS > 3**		
VEGFR2					
IS = 0	116	44	11		
1 < IS < 3	7/20 (35.0%)	9/20 (45.0%)	4/20 (20.0%)	0.000	0.489
IS > 3	0/9 (0.0%)	0/9 (0.0%)	9/9 (100.0%)		

Abbreviations: GLI1 = glioma-associated oncogene homolog 1 proteins; IS = immunoreactive score; TNBC = triple-negative breast cancer; VEGFR2 = vascular endothelial growth factor receptor 2.

showing VEGFR2 $IS>3$, all showed $IS>3$ also for GLI1 (100.0%). Statistical analysis demonstrated a direct significant association between VEGFR2 and GLI1 expression in TNBC patients ($P=0.000$, R Pearson $=0.489$), as shown in Table 1.

GLI1 is frequently overexpressed in TNBC primary and immortalised cell lines. We investigated the expression of the main Hh pathway transducers in 10 human breast cancer cell lines, 5 ER/PgR+ and/or HER2+ (nTNBC) and 5 ER/PgR− and HER2− (TNBC). None of the cell lines used display mutations in the major Hh signalling components; the molecular features of the selected cell lines are depicted in Supplementary Table S4. The expression of SMO and mostly GLI1 was higher in TNBC cell lines (Figure 2A). Similar results have been obtained in primary breast cancer cell lines, generated from two ER+ breast cancer patients and two triple-negative ones: overexpression of GLI1, as well as of its truncated form tGLI1, was also evident in these models

(Figure 2B). The HH pathway ligands Desert Hedgehog, Indian Hedgehog and SHH showed comparable expression in all the analysed cancer cell lines (Supplementary Figure S1). Interestingly, the triple-negative condition seems to influence tumour angiogenesis, as demonstrated by capillary tube formation assay performed using HUVEC cells grown in CM from cultured MDA-MB-361 (nTNBC) or MDA-MB-468 (TNBC) cells. Medium from TNBC cells strongly promoted the endothelial cells ability to form capillary structures; the stimulation was comparable to that obtained by treatment with VEGF-A (Figure 2C). In order to better evaluate the effect of tumour cells on endothelial cell proliferation, co-cultures of mouse bEND5 and breast cancer cell lines were performed. As shown in Figure 2D, TNBC cells promoted bEND5 proliferation in a stronger manner than nTNBC; consistent with this finding, TNBC cell lines (Figure 2E), as well as TNBC primary cells, (Figure 2F) secreted higher levels of VEGF-A compared to nTNBC ones.

Hh pathway regulates the production of pro- and anti-angiogenic secreted factors. To investigate the putative role of Hh activation in TNBC-dependent regulation of tumour angiogenesis, the effects of Hh pathway inhibition on angiogenesis have been compared with those obtained with bevacizumab, a humanised anti-VEGF mAb (Ferrara et al, 2004). To this aim, we used the selective SMO antagonist NVP-LDE225, a clinically approved drug for the treatment of basal cell carcinoma (Rudin, 2012; Sekulic et al, 2012). A capillary tube formation assay was performed using HUVEC cells grown in the conditioned medium of MDA-MB-468 treated with NVP-LDE225 or bevacizumab: NVP-LDE225 treatment discouraged endothelial cells organisation in capillary tubes in a more effective manner than bevacizumab
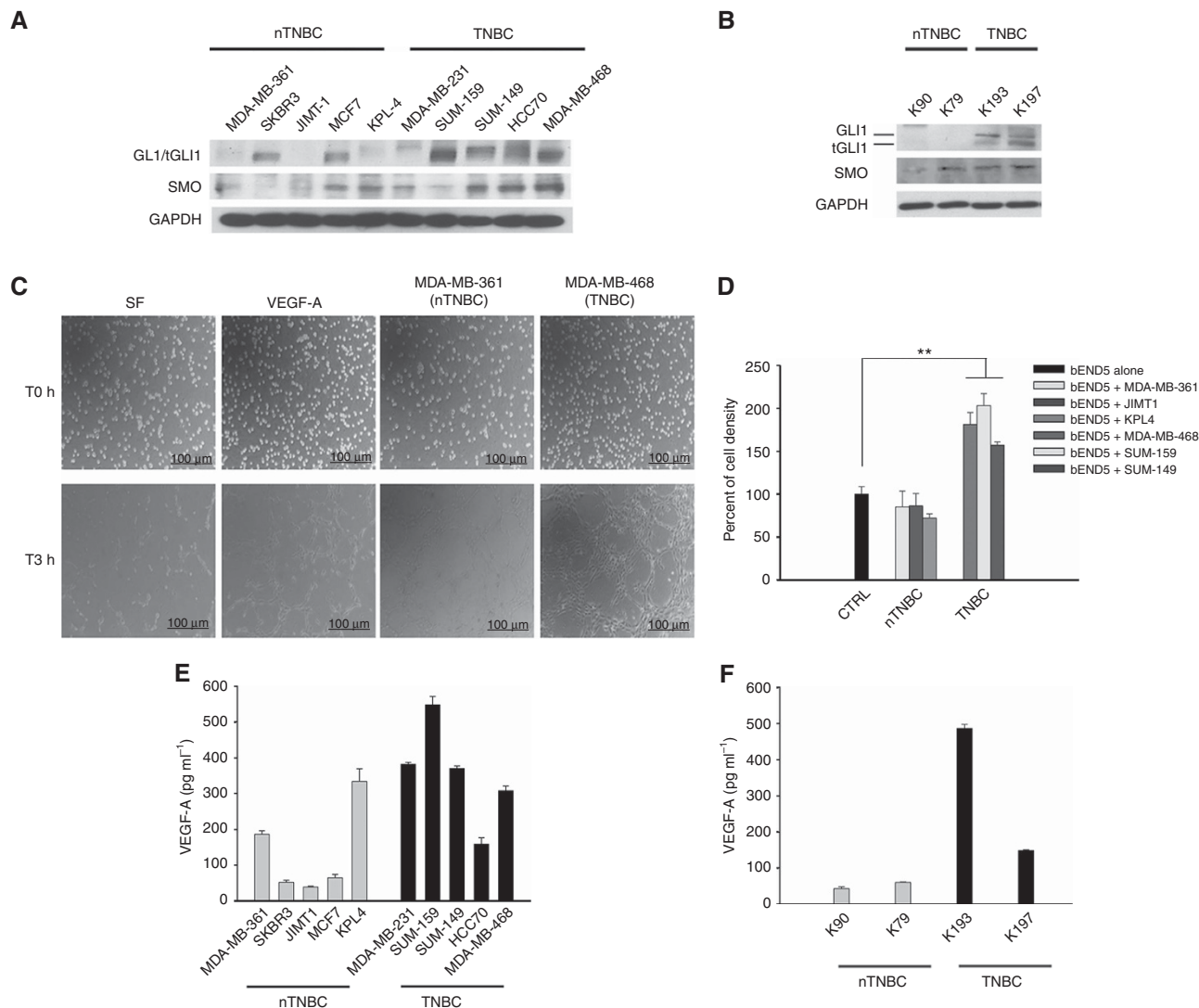
Figure 2. GLI1 is frequently overexpressed in TNBC primary and immortalised cell lines. (**A**, **B**) Western blot analysis of protein expression in a panel of **A** nTNBC or TNBC immortalised cell lines, and (**B**) nTNBC or TNBC primary cell lines. (**C**) Capillary tubes formation assay on HUVEC cells grown on Matrigel in: RPMI serum-free medium; RPMI serum-free medium supplemented with VEGF-A (100 ng ml^{-1}); conditioned growth media from nTNBC (MDA-MB-361) or TNBC (MDA-MB-468). Cells were observed under an inverted microscope, and pictures were taken at T0 hours and after 3 h. Scale bars, 100 μm. (**D**) Percent of cell density of bEND5 endothelial cells co-cultured with nTNBC or TNBC cells for 3 days, as measured by MTT assay. Data represent the mean ($\pm$ s.d.) of three independent experiments, each performed in triplicate. (**E**, **F**) ELISA assay for the determination of VEGF-A concentrations (pg ml^{-1}) in conditioned media from (**E**) nTNBC or TNBC immortalised cells, or (**F**) primary cells. Data represent the mean ($\pm$ s.d.) of three independent experiments, each performed in triplicate. Bars, s.d. Asterisks indicate statistical significance, as determined by the Student t-test (**$P < 0.01$).

(Figure 3A). Conversely, bevacizumab determined a reduced presence of secreted VEGFA in culture medium compared to NVP-LDE225 treatment, as shown in Figure 3B.

The paracrine effect of Hh pathway inhibition by NVP-LDE225 on tumour microenvironment was also evaluated *in vivo*, in Balb/C nude mice orthotopically xenografted with MDA-MB-468 cells and treated with NVP-LDE225 or bevacizumab. Two weeks after starting treatments, mice were killed, and the expression of the angiogenic marker CD31 on tumour tissue was evaluated through immunofluorescence analysis (Supplementary Figure S2). NVP-LDE225 appears to be more effective in inhibiting angiogenesis than bevacizumab.

On the basis of these data, we hypothesised that Hh inhibition could lead to dysregulation of some uncharacterised secreted factors, able to regulate tumour angiogenesis. Therefore, a multiplex ELISA assay for 16 secreted factors was conducted on TNBC media upon treatment of TNBC cultured cells with NVP-LDE225.

Levels of sVEGFR2 and THBS1 significantly increased in TNBC cell supernatants after NVP-LDE225 treatment (Figure 3C and D); sVEGFR2 and THBS1 mRNA levels were augmented as well (Figure 3E and F). These data have been confirmed by ELISA assays specific for each analyte (data not shown). These findings are of interest since sVEGFR2 and THBS1 are known as two endogenous angiogenesis and lymphangiogenesis inhibitors (Nyberg *et al*, 2005).

GLI1 regulates VEGFR2 expression. To investigate the capability of Hh pathway to modulate components of the angiogenic machinery, expression of VEGFR2 has been measured: after treatment with NVP-LDE225 a reduction of protein and mRNA levels was observed in both MDA-MB-468 and HUVEC cells (Figure 4A and B), an event paired with a simultaneous reduction of NRP2, as already known (Goel *et al*, 2013). Therefore, we hypothesised that Hh could be involved in the transcriptional
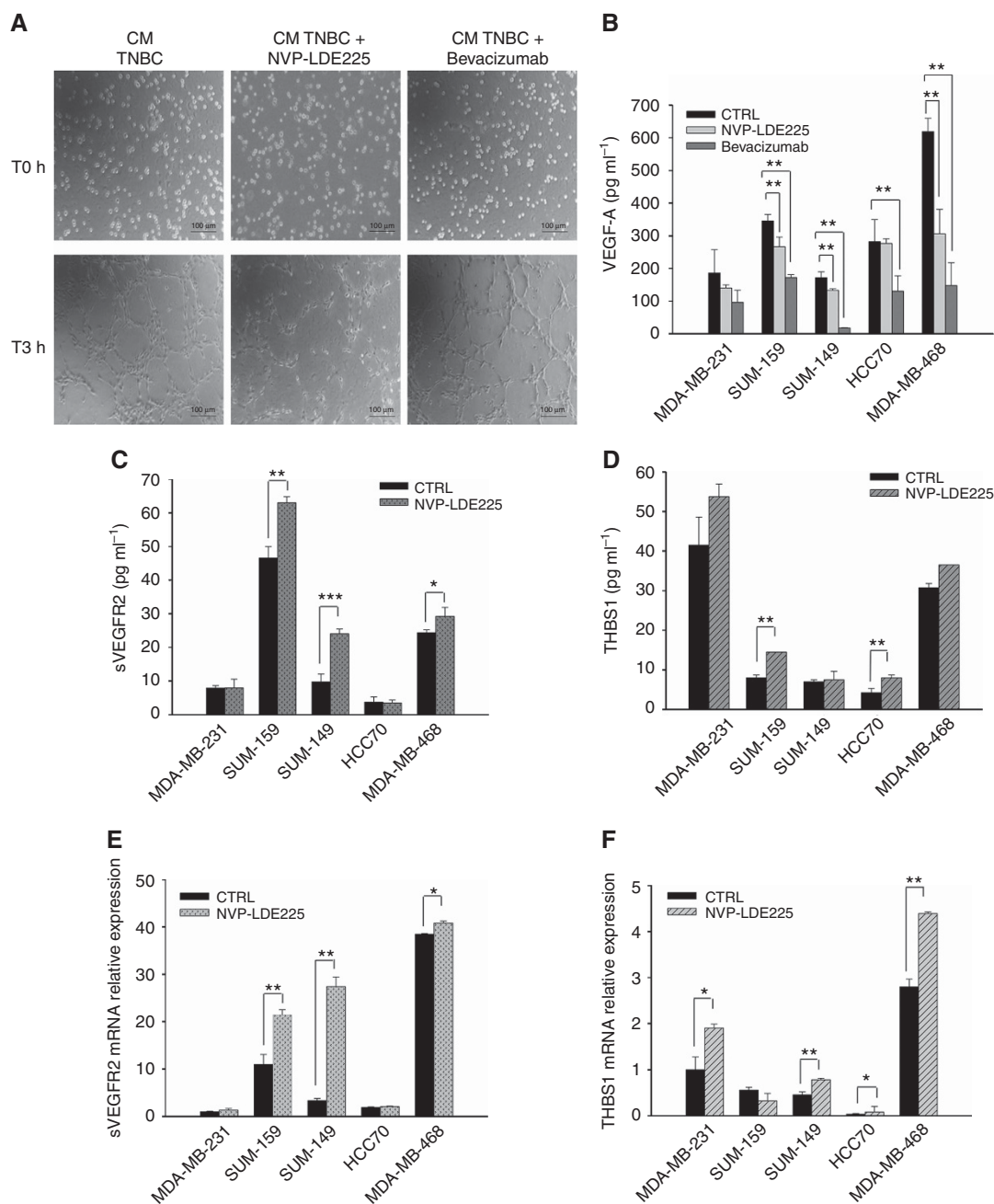
Figure 3. Hh pathway regulates the production of pro- and anti-angiogenic secreted factors. (**A**) Capillary tubes formation assay on HUVEC cells grown on Matrigel in the presence of conditioned growth media of TNBC (MDA-MB-468) cells treated with NVP-LDE225 (2.5 μM) or bevacizumab (1 μM).Cells were observed under an inverted microscope, and pictures were taken at T0 hours and after 3 h. Scale bars, 100 μm. (**B**) Quantitative analysis of VEGF-A in conditioned media (CM) of MDA-MB-231, SUM-159, SUM-149, HCC70 and MDA-MB-468 cells treated with NVP-LDE225 (2.5 μM) or bevacizumab (1 μM). (**C**, **D**) Quantitative analysis of (**C**) sVEGFR2 and (**D**) THBS1 in CM of MDA-MB-231, SUM-159, SUM-149, HCC70 and MDA-MB-468 cells treated with NVP-LDE225 (2.5 μM), as performed by using a multiplexed immunoassay. (**E**, **F**) Relative expression of (**E**) sVEGFR2 and (**F**) THBS1 mRNA in MDA-MB-231, SUM-159, SUM-149, HCC70 and MDA-MB-468 treated with NVP-LDE225 (2.5 μM), as performed by real-time RT–PCR (qRT-PCR) analysis. Data were calculated with mean cycle threshold (CT) values, normalised to endogenous control. Data represent the mean (± s.d.) of three independent experiments, each performed in triplicate. Bars, s.d. Asterisks indicate statistical significance, as determined by the Student t-test (*$P < 0.05$, **$P < 0.01$, ***$P < 0.001$).

modulation of the VEGFR2 receptor, eventually mediated by GLI1. To address this issue, GLI1/tGLI1 silencing was performed in MDA-MB-468 and HUVEC cells using a siRNA pool for all GLI1 forms. As depicted in Figure 4C, GLI1 silencing caused down-regulation of VEGFR2 protein expression. Then GLI1 and tGLI1 overexpressions were performed in MDA-MB-231, a TNBC cell line with a low endogenous expression of GLI1. The levels of VEGFR2 protein augmented when tGLI1 was overexpressed, as

shown in Figure 4D. A bioinformatics analysis looking for a known GLI1/tGLI1-binding site (Kinzler and Vogelstein, 1990) revealed two putative sequences within ≈500 bp upstream of VEGFR2 transcription start site (Supplementary Figure S3). Therefore, we carried out a luciferase reporter assay. As shown in Figure 4E, VEGFR2 gene promoter is activated in GLI1 overexpressing MDA-MB-468 cells, and NVP-LDE225 treatment significantly abrogates its activity (P-value < 0.001). To further validate the functional

GLI1/VEGFR2 promoter interaction, we performed a ChIP analysis followed by PCR amplification of four different regions (P1–P4) of VEGFR2 gene promoter (Supplementary Figure S3).

We found that tGLI1 binds the VEGFR2 promoter, especially in the P3 region, confirming that tGLI1 transcriptionally enhances VEGFR2 (Figure 4F). The graphical representation of tGLI1-
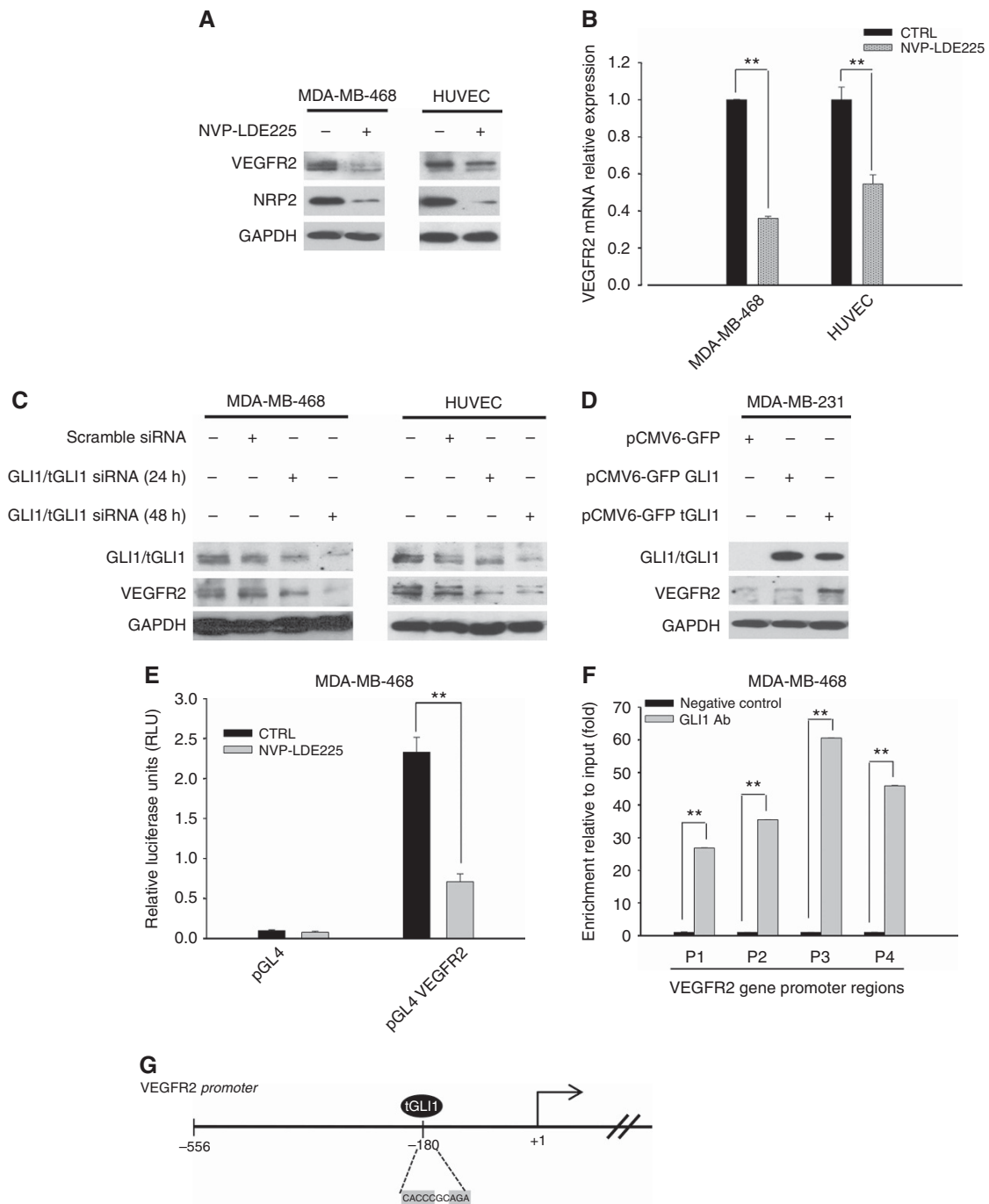

Figure 4. GLI1 regulates VEGFR2 expression. (A) Western blot analysis of protein expression in MDA-MB-468 and HUVEC cells treated with NVP-LDE225 (2.5 μM). (B) Relative expression of sVEGFR2 mRNA in MDA-MB-468 and HUVEC cells treated with NVP-LDE225 (2.5 μM), as performed by real-time RT–PCR (qRT-PCR) analysis. Data were calculated with mean cycle threshold (CT) values, normalised to endogenous control. Data represent the mean ($\pm$ s.d.) of three independent experiments, each performed in triplicate. (C) Western blot analysis of protein expression in MDA-MB-468 and HUVEC cells, 24 and 48 h after transfection with scramble or GLI1 siRNA pool (50 nmol l^{-1}) using DharmaFECT 1 Transfection Reagent in DMEM. (D) Western blot analysis of protein expression in MDA-MB-231 cells, 24 h after transfection with either pCMV6-GFP empty vector, pCMV6-GFP GLI1 or pCMV6-GFP tGLI1 plasmids using lipofectamine 2000 in DMEM. (E) Relative luciferase units in MDA-MB-468 cells transfected with the empty pGL4 plasmid or the pGL4 plasmid containing 500 bp fragment of VEGFR2 promoter, and treated with NVP-LDE225 5 μM for 24 h after transfection. Luciferase activity was determined 48 h after transfection. Results were the average of three independent experiments. (F) Chromatin immunoprecipitation (ChIP) assay in MDA-MB-468 cells by using a GLI1 antibody and primers specific for the VEGFR2 promoter. Results were reported as fold change compared to negative control (no antibody); results were the average of three independent experiments. Bars, s.d. Asterisks indicate statistical significance, as determined by the Student t-test (**$P<0.01$). (G) Graphical representation of VEGFR2 proximal promoter region, containing the binding site of tGLI1 indicated by oval.

binding site on VEGFR2 promoter region is shown in the Figure 4G. The downregulation of VEGFR2 observed upon NVP-LDE225 could be related to an interference with GLI1 intracellular localisation, since NVP-LDE225 can reduce nuclear translocation of GLI1 and to increase its cytoplasmic retention, as demonstrated by western blot and immunofluorescence assays (Supplementary Figure S4).

NVP-LDE225 increases the efficacy of paclitaxel in nude mice xenografted with TNBC tumours. Pharmacological inhibition of Hh *in vitro* simultaneously reduces the expression of pro-angiogenic receptors and increases the production of anti-angiogenic secreted factors both in endothelial and TNBC cells. To analyse the overall effect of these findings, an *in vivo* experiment was performed in Balb/C nude mice orthotopically xenografted with MDA-MB-468 cells. We compared the effects of NVP-LDE225 with bevacizumab, each of them combined with paclitaxel; the last combination represents the current standard of care for TNBC patients (Herold and Anders, 2013). As reported in Figure 5A, untreated mice reached the maximum allowed tumour size, *ca.* 2 cm^3, on day 63; at this time point, NVP-LDE225 plus paclitaxel and bevacizumab plus paclitaxel produced 55 and 29% of growth inhibition, respectively. Notably, the combination of NVP-LDE225 and paclitaxel caused a long-lasting antitumour activity, with a tumour size of 1.64 cm^3 at the end of the experiment, whereas bevacizumab plus paclitaxel-treated mice reached the maximum allowed tumour size on day 84. Comparison of tumour sizes, evaluated by the one-way ANOVA test, was statistically significant for the combination NVP-LDE225 and paclitaxel *vs* control ($P \leqslant 0.05$; Figure 5A). Consistently, as shown in Figure 5B, mice treated with NVP-LDE225 and paclitaxel showed a slightly prolonged median survival compared with those treated with bevacizumab and paclitaxel, since 20% of NVP-LDE225 paclitaxel-treated mice was still alive at the end of the experiment. Median survival in the NVP-LDE225 plus paclitaxel-treated mice was significantly longer than in control mice (79.50 *vs* 53.50 days, $P = 0.0089$; Figure 5B; Supplementary Table S5). NVP-LDE225-based treatment was well tolerated; no weight loss or other signs of acute or delayed toxicity were observed. Western blot analysis of tumours from mice killed on day 21, after 2 weeks of treatment, demonstrated that NVP-LDE225 combined with paclitaxel efficiently interfered with Hh-dependent signal transduction by reducing the expression of cyclin D1 and Bcl2, both direct targets of GLI1 (Figure 5C). Interestingly, NVP-LDE225 plus paclitaxel treatment was effective in reducing VEGFR2 and augmenting sVEGFR2 expression, consistently with *in vitro* findings (Figure 5C). Furthermore, NVP-LDE225 combined with paclitaxel was able to reduce human VEGF-A in mice serum (Figure 5D). Conversely, an overexpression of THBS1 was found in sera collected from NVP-LDE225 plus paclitaxel-treated mice (Figure 5E). The treatment induced sVEGFR2 secretion by both stromal (mouse sVEGFR2) and tumour cells (human sVEGFR2; Figure 5F and G).

Immunoistochemical analysis on tumours from mice killed on day 21, after 2 weeks of treatment, demonstrated that NVP-LDE225 combined with paclitaxel interferes with angiogenesis in nude mice xenografted with TNBC tumours. In fact, the combination NVP-LDE225 plus paclitaxel reduced the expression of VEGFR2, NRP2 and CD31, as well as of the proliferation marker Ki67, more efficiently than the combination bevacizumab plus paclitaxel (Supplementary Figure S5).

DISCUSSION

Breast cancers, which lack the expression of ER, PgR and HER2 receptors, are grouped and defined as TNBCs. Owing to the lack of targeted therapies, these cancers are uniformly treated with chemotherapy (Cleator *et al*, 2007); nevertheless, outcomes are poor compared with those of other subtypes (Mustacchi and De Laurentiis, 2015). Despite considered a single entity from a clinical perspective, TNBC is a heterogeneous disease, which comprises distinct molecular subtypes, a condition that urgently needs the development of novel treatment strategies (Bose, 2015). Thus, recent research efforts have focused on identifying TNBC subtypes bearing uniformly actionable molecular features (Shah *et al*, 2012).

Higher expression of different biomarkers, including VEGFR, epidermal growth factor receptor and fibroblast growth factor receptor, has given the rationale for clinical trials assessing the role of targeted inhibitors to these pathways in triple-negative tumours (Andreopoulou *et al*, 2015). Results from these trials have shown some benefit in small subgroups of patients, which reflects the heterogeneity of TNBC (Arnedos *et al*, 2012) and highlights the need for a further sub-classification of these tumours for better prognosis assessment and treatment individualisation.

Several studies suggest the involvement of Hh pathway in breast cancer (O'Toole *et al*, 2011), although the functional significance of these findings and their potential therapeutic impact is unclear. In our work, we found that TNBC cells overexpress the Hh family transcription factors GLI1 and tGLI1. In a tissue microarray analysis on 200 TNBC patients, about 12 and 26% of patients expressed the GLI1 protein at low and moderate levels, respectively. Interestingly, a statistically significant association between VEGFR2 and GLI1 expression was found in TNBC patients.

On the basis of this evidence, since it is known that the Hh pathway promotes cancer through epithelial–stromal interaction (Yauch *et al*, 2008; Theunissen and de Sauvage, 2009; Heller *et al*, 2012), we explored the effect of GLI1/tGLI1 overexpression in TNBC on the endothelial compartment and TNBC initiated angiogenesis. Overexpressing GLI1 cancer cells influenced endothelial cells proliferation and their capability to form capillary, in part regulating the VEGF-A production as previously described. Despite Hh inhibition depressed VEGF-A secretion less efficiently than the anti-VEGF mAb bevacizumab, we found that NVP-LDE225 discouraged capillary organisation in a more evident manner. With the intent to demonstrate that the Hh pathway could regulate tumour angiogenesis in both VEGF-dependent and VEGF-independent manners, we found an upregulation of sVEGFR2 and THBS1 after pharmacological Hh pathway inhibition. Soluble VEGFR2 represents a VEGFR2 splicing variant identified as an endogenous inhibitor of lymphangiogenesis; it acts as a decoy receptor, sequestering VEGF from VEGFR2 binding (Albuquerque *et al*, 2009; Shibata *et al*, 2010). Thrombospondin1 represents a natural anti-angiogenic secreted factor (Lawler, 2002; Henkin and Volpert, 2011). Collectively, the reduction of VEGF-A, coupled with the upregulation of sVEGFR2 and THBS1, could explain the deeper anti-angiogenic *in vitro* effect of NVP-LDE225 compared to bevacizumab, since the latter is able to only suppress VEGF-A-activated angiogenesis. Simultaneously with the increase of sVEGFR2, reduced levels of VEGFR2 protein and mRNA were found after Hh inhibition, thus suggesting a putative regulation of VEGFR2 expression by Hh. As hypothesised by bioinformatics analysis, we demonstrated a functional interaction between tGLI1 and the VEGFR2 promoter, demonstrating a transcriptional modulation of the VEGFR2 receptor mediated by tGLI1.

These findings suggest that GLI1/tGLI1 overexpressing cancer cells promote tumour progression in a paracrine manner. They can orchestrate tumour vascularisation not only by inducing VEGF-A secretion but also by upregulating VEGFR2 on cancer cell surface, thus establishing a secreted factors/receptors autocrine loop. The Hh pathway could regulate other angiogenic receptors: for instance, Goel *et al* (2013) demonstrated that GLI1 sustains a NRP2/$\alpha6\beta1$ integrin-based autocrine loop through enhanced NRP2 expression. Increased production of THBS1 and sVEGFR2 strengthens the anti-angiogenic effects observed upon Hh
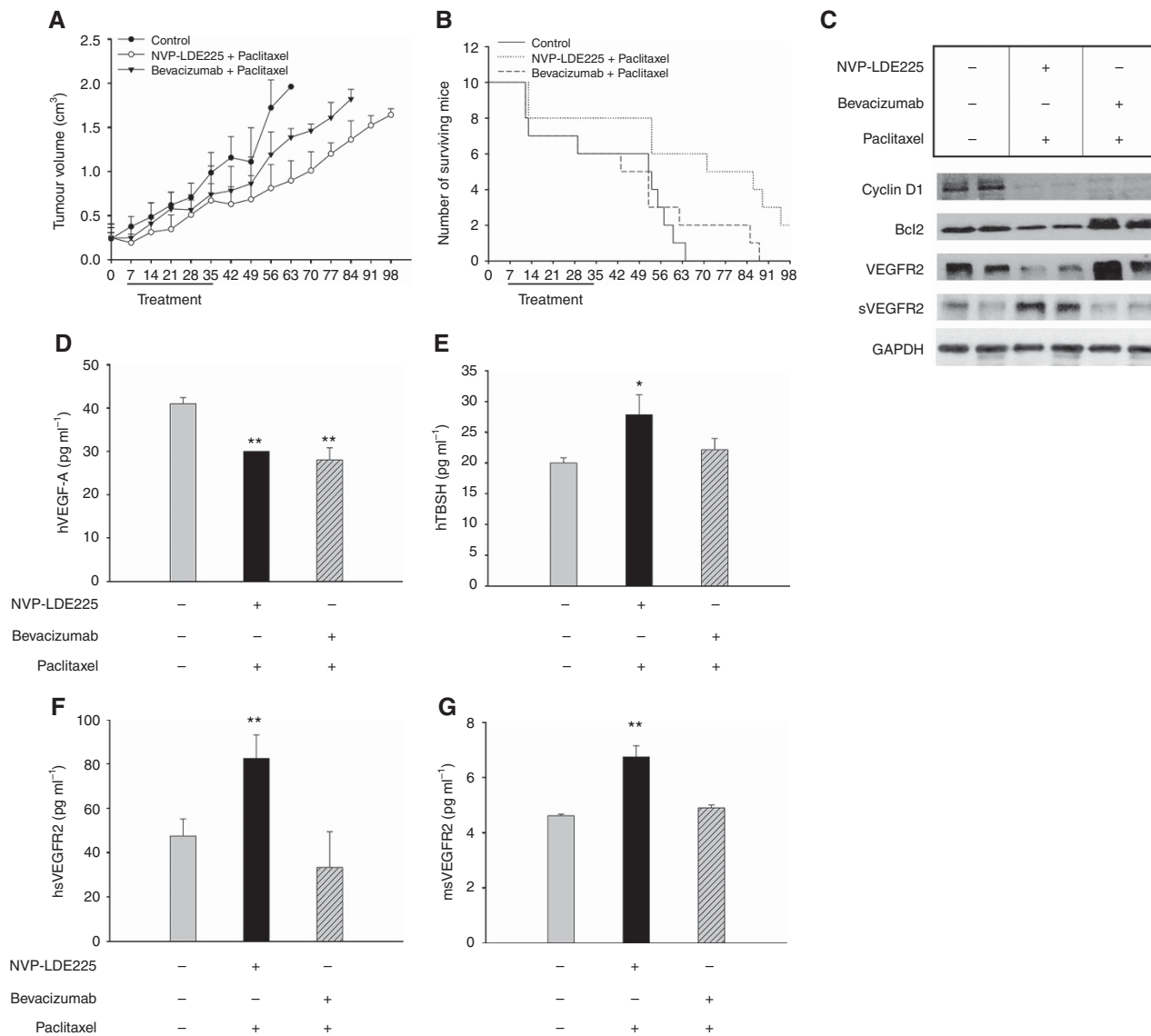
Figure 5. NVP-LDE225 increases the efficacy of paclitaxel in nude mice xenografted with TNBC tumours. (**A**) Tumour volume of MDA-MB-468 orthotopic xenografts in nude mice, randomised (10 per group) to receive NVP-LDE225 or bevacizumab in combination with paclitaxel, as described in the Methods section. The one-way ANOVA test was used to compare tumour sizes among treatment groups at the median survival time of the control group (35 days). Comparison of tumour sizes, evaluated by the one-way ANOVA test, was statistically significant for the combination NVP-LDE225 and paclitaxel *vs* control ($P \leqslant 0.05$). (**B**) Number of surviving mice orthotopically xenografted with MDA-MB-468, after treatments with NVP-LDE225 or bevacizumab in combination with paclitaxel, as described in the Methods section. Median survival differences were statistically significant median survival in the NVP-LDE225 plus paclitaxel-treated mice was significantly longer than in control mice (79.50 *vs* 53.50 days, $P = 0.0089$, log-rank test). (**C**) Western blot analysis on total lysates from MDA-MB-468 tumour specimens of mice killed on day 21, after 2 weeks of treatment with NVP-LDE225 or bevacizumab in combination with paclitaxel. (**D**, **E**, **F**, **G**) ELISA assay for the determination of (**D**) hVEGF-A, (**E**) hTHSB1, (**F**) h-sVEGFR2 and (**G**) m-sVEGFR2 concentrations (pg ml^{-1}) in mice sera, collected on day 21. Data represent the mean ($\pm$ s.d.) of three independent experiments, each performed in triplicate. Bars, s.d. Asterisks indicate statistical significance, as determined by the Student *t*-test (*$P < 0.05$, **$P < 0.01$).

inhibition. Collectively, our data suggest that Hh pathway can regulate tumour angiogenesis at multiple levels (Supplementary Figure S6). Therefore, it is possible that Hh pharmacological inhibition discourages the pro-angiogenic behaviour of TNBC.

These data are in part confirmed by the finding that, in tumour samples of TNBC patients, VEGFR2 expression correlated with GLI1 expression. This co-expression reflects the functional connection between the transcription factor and the receptor identified in *in vitro* analysis. Therefore, co-expressing GLI1 and VEGFR2 TNBC might be considered a new subgroup in which Hh

pathway inhibition could be clinically investigated because of its effects on both cancer cells and tumour microenvironment.

To evaluate the translational relevance of these findings, the combinations of paclitaxel with either NVP-LDE225 or bevacizumab were tested in TNBC xenografted mice. Whereas bevacizumab administration remains controversial, especially because of small clinical benefits and high costs associated, its combination with paclitaxel represents the canonical schedule for TNBC treatment. By scheduling NVP-LDE225 rather than bevacizumab, we attempted to demonstrate the therapeutic advantage of this

combination. In line with the findings that NVP-LDE225 seems to act as a multi anti-angiogenic drug, modulating both secreted factors and receptors involved in angiogenesis, mouse serum levels of circulating VEGF-A were decremented upon NVP-LDE225 administration. In addition, the treatment induced an over-production of THBS1 from tumour cells and of sVEGFR2 from both tumour (h-sVEGFR2) and endothelial (m-sVEGFR2) cells, events associated with discouraged neovascularisation and meta-static potential inhibition (Albuquerque *et al*, 2009; Henkin and Volpert, 2011). Vascular endothelial growth factor receptor 2 levels on tumour surface were deeply reduced as well as some proliferation markers such as pERK. Collectively, the combination of NVP-LDE225 and paclitaxel provides a better sustained inhibition of both tumour cells proliferation and endothelial cells organisation.

Our data support the clinical development of novel pharmaco-logical combinations that include Hh blockade, especially those that could potentiate anti-angiogenic effects: Hh inhibitors could overcome the limitations of bevacizumab use, by acting simulta-neously against tumour growth and angiogenesis formation. To date, few clinical trials with Hh inhibitors have allowed the enrolment of TNBC patients; among them, only the NCT02027376 phase Ib trial is currently evaluating the combination of NVP-LDE225 and docetaxel in this subgroup of breast cancer patients (www.clinicaltrials.gov, Identifier: NCT0202737647).

ACKNOWLEDGEMENTS

CONFLICT OF INTEREST

The authors declare no conflict of interest.

REFERENCES

Albuquerque RJ, Hayashi T, Cho WG, Kleinman ME, Dridi S, Takeda A, Baffi JZ, Yamada K, Kaneko H, Green MG, Chappell J, Wilting J, Weich HA, Yamagami S, Amano S, Mizuki N, Alexander JS, Peterson ML, Brekken RA, Hirashima M, Capoor S, Usui T, Ambati BK, Ambati J (2009) Alternatively spliced vascular endothelial growth factor receptor-2 is an essential endogenous inhibitor of lymphatic vessel growth. *Nat Med* **15**: 1023–1030.

André F, Job B, Dessen P, Tordai A, Michiels S, Liedtke C, Richon C, Yan K, Wang B, Vassal G, Delaloge S, Hortobagyi GN, Symmans WF, Lazar V, Pusztai L (2009) Molecular characterization of breast cancer with high-resolution oligonucleotide comparative genomic hybridization array. *Clin Cancer Res* **15**: 441–451.

Andreopoulou E, Schweber SJ, Sparano JA, McDaid HM (2015) Therapies for triple negative breast cancer. *Expert Opin Pharmacother* **16**: 983–998.

Angelucci C, Maulucci G, Lama G, Proietti G, Colabianchi A, Papi M, Maiorana A, De Spirito M, Micera A, Balzamino OB, Di Leone A, Masetti R, Sica G (2012) Epithelial-stromal interactions in human breast cancer: effects on adhesion, plasma membrane fluidity and migration speed and directness. *PLoS One* **7**: e50804.

Arnedos M, Bihan C, Delaloge S, Andre F (2012) Triple-negative breast cancer: are we making headway at least? *Ther Adv Med Oncol* **4**: 195–210.

Bear HD, Tang G, Rastogi P, Geyer Jr CE, Robidoux A, Atkins JN, Baez-Diaz L, Brufsky AM, Mehta RS, Fehrenbacher L, Young JA, Senecal FM, Gaur R, Margolese RG, Adams PT, Gross HM, Costantino JP, Swain SM, Mamounas EP, Wolmark N (2012) Bevacizumab added to neoadjuvant chemotherapy for breast cancer. *N Engl J Med* **366**: 310–320.

Bose S (2015) Triple-negative breast carcinoma: morphologic and molecular subtypes. *Adv Anat Pathol* **22**: 306–313.

Cao X, Geradts J, Dewhirst MW, Lo HW (2012) Upregulation of VEGF-A and CD24 gene expression by the tGLI1 transcription factor contributes to the aggressive behavior of breast cancer cells. *Oncogene* **31**: 104–115.

Carpenter RL, Lo HW (2012) Hedgehog pathway and GLI1 isoforms in human cancer. *Discov Med* **13**: 105–113.

Chacón RD, Costanzo MV (2010) Triple-negative breast cancer. *Breast Cancer Res* **12**(Suppl 2): S3.

Cleator S, Heller W, Coombes RC (2007) Triple-negative breast cancer: therapeutic options. *Lancet Oncol* **8**: 235–244.

Cohen Jr MM (2010) Hedgehog signaling update. *Am J Med Genet A* **152A**: 1875–1914.

D'Amato C, Rosa R, Marciano R, D'Amato V, Formisano L, Nappi L, Raimondo L, Di Mauro C, Servetto A, Fulciniti F, Cipolletta A, Bianco C, Ciardiello F, Veneziani BM, De Placido S, Bianco R (2014) Inhibition of Hedgehog signalling by NVP-LDE225 (Erismodegib) interferes with growth and invasion of human renal cell carcinoma cells. *Br J Cancer* **111**: 1168–1179.

Dent R, Trudeau M, Pritchard KI, Hanna WM, Kahn HK, Sawka CA, Lickley LA, Rawlinson E, Sun P, Narod SA (2007) Triple-negative breast cancer: clinical features and patterns of recurrence. *Clin Cancer Res* **13**: 4429–4434.

Ferrara N, Hillan KJ, Gerber HP, Novotny W (2004) Discovery and development of bevacizumab, an anti-VEGF antibody for treating cancer. *Nat Rev Drug Discov* **3**: 391–400.

Goel HL, Pursell B, Chang C, Shaw LM, Mao J, Simin K, Kumar P, Vander Kooi CW, Shultz LD, Greiner DL, Norum JH, Toftgard R, Kuperwasser C, Mercurio AM (2013) GLI1 regulates a novel neuropilin-2/a6b1 integrin based autocrine pathway that contributes to breast cancer initiation. *EMBO Mol Med* **5**: 488–508.

Gray R, Bhattacharya S, Bowden C, Miller K, Comis RL (2009) Independent review of E2100: a phase III trial of bevacizumab plus paclitaxel versus paclitaxel in women with metastatic breast cancer. *J Clin Oncol* **27**(30): 4966–4972.

Habib JG, O'Shaughnessy JA (2016) The Hedgehog pathway in triple-negative breast cancer. *Cancer Med* **5**: 2989–3006.

Haffty BG, Yang Q, Reiss M, Kearney T, Higgins SA, Weidhaas J, Harris L, Hait W, Toppmeyer D (2006) Locoregional relapse and distant metastasis in conservatively managed triple negative early-stage breast cancer. *J Clin Oncol* **24**: 5652–5657.

Harris LG, Pannell LK, Singh S, Samant RS, Shevde LA (2012) Increased vascularity and spontaneous metastasis of breast cancer by Hedgehog signaling mediated upregulation of cyr61. *Oncogene* **31**: 3370–3380.

Heller E, Hurchla MA, Xiang J, Su X, Chen S, Schneider J, Joeng KS, Vidal M, Goldberg L, Deng H, Hornick MC, Prior JL, Piwnica-Worms D, Long F, Cagan R, Weilbaecher KN (2012) Hedgehog signaling inhibition blocks growth of resistant tumors through effects on tumor microenvironment. *Cancer Res* **72**: 897–907.

Henkin J, Volpert OV (2011) Therapies using anti-angiogenic peptide mimetics of thrombospondin-1. *Expert Opin Ther Targets* **15**: 1369–1386.

Herold CI, Anders CK (2013) New targets for triple-negative breast cancer. *Oncology (Williston Park)* **27**: 846–854.

Katoh Y, Katoh M (2009) Hedgehog target genes: mechanisms of carcinogenesis induced by aberrant Hedgehog signaling activation. *Curr Mol Med* **9**: 873–886.

Kinzler KW, Vogelstein B (1990) The *GLI* gene encodes a nuclear protein which binds specific sequences in the human genome. *Mol Cell Biol* **10**: 634–642.

Lawler J (2002) Thrombospondin-1 as an endogenous inhibitor of angiogenesis and tumor growth. *J Cell Mol Med* **6**: 1–12.

Liedtke C, Mazouni C, Hess KR, André F, Tordai A, Mejia JA, Symmans WF, Gonzalez-Angulo AM, Hennessy B, Green M, Cristofanilli M, Hortobagyi GN, Pusztai L (2008) Response to neoadjuvant therapy and long-term survival in patients with triple-negative breast cancer. *J Clin Oncol* **26**: 1275–1281.

Linderholm BK, Hellborg H, Johansson U, Elmberger G, Skoog L, Lehtiö J, Lewensohn R (2009) Significantly higher levels of vascular endothelial growth factor (VEGF) and shorter survival times for patients with primary operable triple-negative breast cancer. *Ann Oncol* **20**: 1639–1646.

Miles DW, Chan A, Dirix LY, Cortés J, Pivot X, Tomczak P, Delozier T, Sohn JH, Provencher L, Puglisi F, Harbeck N, Steger GG, Schneeweiss A, Wardley AM, Chlistalla A, Romieu G (2010) Phase III study of bevacizumab plus docetaxel compared with placebo plus docetaxel for the first-line treatment of human epidermal growth factor receptor 2-negative metastatic breast cancer. *J Clin Oncol* **28**: 3239–3247.

Mohammed RA, Ellis IO, Mahmmod AM, Hawkes EC, Green AR, Rakha EA, Martin SG (2011) Lymphatic and blood vessels in basal and triple-negative breast cancers: characteristics and prognostic significance. *Mod Pathol* **24**: 774–785.

Mustacchi G, De Laurentiis M (2015) The role of taxanes in triple-negative breast cancer: literature review. *Drug Des Devel Ther* **9**: 4303–4318.

Nagase T, Nagase M, Machida M, Fujita T (2008) Hedgehog signalling in vascular development. *Angiogenesis* **11**: 71–77.

Nyberg P, Xie L, Kalluri R (2005) Endogenous inhibitors of angiogenesis. *Cancer Res* **65**: 3967–3979.

O'Toole SA, Machalek DA, Shearer RF, Millar EK, Nair R, Schofield P, McLeod D, Cooper CL, McNeil CM, McFarland A, Nguyen A, Ormandy CJ, Qiu MR, Rabinovich B, Martelotto LG, Vu D, Hannigan GE, Musgrove EA, Christ D, Sutherland RL, Watkins DN, Swarbrick A (2011) Hedgehog overexpression is associated with stromal interactions and predicts for poor outcome in breast cancer. *Cancer Res* **71**: 4002–4014.

Pak E, Segal RA (2016) Hedgehog signal transduction: key players, oncogenic drivers, and cancer therapy. *Dev Cell* **38**: 333–344.

Palma G, Frasci G, Chirico A, Esposito E, Siani C, Saturnino C, Arra C, Ciliberto G, Giordano A, D'Aiuto M (2015) Triple negative breast cancer: looking for the missing link between biology and treatments. *Oncotarget* **6**: 26560–26574.

Penault-Llorca F, Viale G (2012) Pathological and molecular diagnosis of triple-negative breast cancer: a clinical perspective. *Ann Oncol* **23**: vi19–vi22.

Riku M, Inaguma S, Ito H, Tsunoda T, Ikeda H, Kasai K (2016) Down-regulation of the zinc-finger homeobox protein TSHZ2 releases GLI1 from the nuclear repressor complex to restore its transcriptional activity during mammary tumorigenesis. *Oncotarget* **7**: 5690–5701.

Robert NJ, Diéras V, Glaspy J, Brufsky AM, Bondarenko I, Lipatov ON, Perez EA, Yardley DA, Chan SY, Zhou X, Phan SC, O'Shaughnessy J (2011) RIBBON-1: randomized, double-blind, placebo-controlled, phase III trial of chemotherapy with or without bevacizumab for first-line treatment of human epidermal growth factor receptor 2-negative, locally recurrent or metastatic breast cancer. *J Clin Oncol* **29**: 1252–1260.

Rohatgi R, Milenkovic L, Corcoran RB, Scott MP (2009) Hedgehog signal transduction by smoothened: pharmacologic evidence for a 2-step activation process. *Proc Natl Acad Sci USA* **106**: 3196–3201.

Rudin CM (2012) Vismodegib. *Clin Cancer Res* **18**: 3218–3222.

Sekulic A, Migden MR, Oro AE, Dirix L, Lewis KD, Hainsworth JD, Solomon JA, Yoo S, Arron ST, Friedlander PA, Marmur E, Rudin CM, Chang AL, Low JA, Mackey HM, Yauch RL, Graham RA, Reddy JC, Hauschild A (2012) Efficacy and safety of vismodegib in advanced basal-cell carcinoma. *N Engl J Med* **366**: 2171–2179.

Shah SP, Roth A, Goya R, Oloumi A, Ha G, Zhao Y, Turashvili G, Ding J, Tse K, Haffari G, Bashashati A, Prentice LM, Khattra J, Burleigh A, Yap D, Bernard V, McPherson A, Shumansky K, Crisan A, Giuliany R, Rosner J, Lai D, Birol I, Varhol R, Tam A, Dhalla N, Zeng T, Ma K, Chan SK, Griffith M, Moradian A, Cheng SW, Morin GB, Watson P, Gelmon K, Chia S, Chin SF, Curtis C, Rueda OM, Pharoah PD, Damaraju S, Mackey J, Hoon K, Harkins T, Tadigotla V, Sigaroudinia M, Gascard P, Tlsty T, Costello JF, Meyer IM, Eaves CJ, Wasserman WW, Jones S, Huntsman D, Hirst M, Caldas C, Marra MA, Aparicio S (2012) The clonal and mutational evolution spectrum of primary triple-negative breast cancers. *Nature* **486**: 395–399.

Shahi MH, Afzal M, Sinha S, Eberhart CG, Rey JA, Fan X, Castresana JS (2010) Regulation of sonic Hedgehog-GLI1 downstream target genes PTCH1, Cyclin D2, Plakoglobin, PAX6 and NKX2.2 and their epigenetic status in medulloblastoma and astrocytoma. *BMC Cancer* **10**: 614.

Shibata MA, Ambati J, Shibata E, Albuquerque RJ, Morimoto J, Ito Y, Otsuki Y (2010) The endogenous soluble VEGF receptor-2 isoform suppresses lymph node metastasis in a mouse immunocompetent mammary cancer. *BMC Med* **8**: 69.

Tao Y, Mao J, Zhang Q, Li L (2011) Overexpression of Hedgehog signaling molecules and its involvement in triple-negative breast cancer. *Oncol Lett* **2**: 995–1001.

Theunissen JW, de Sauvage FJ (2009) Paracrine Hedgehog signaling in cancer. *Cancer Res* **69**: 6007–6010.

Yamazaki M, Nakamura K, Mizukami Y, Ii M, Sasajima J, Sugiyama Y, Nishikawa T, Nakano Y, Yanagawa N, Sato K, Maemoto A, Tanno S, Okumura T, Karasaki H, Kono T, Fujiya M, Ashida T, Chung DC, Kohgo Y (2008) Sonic Hedgehog derived from human pancreatic cancer cells augments angiogenic function of endothelial progenitor cells. *Cancer Sci* **99**: 1131–1138.

Yauch RL, Gould SE, Scales SJ, Tang T, Tian H, Ahn CP, Marshall D, Fu L, Januario T, Kallop D, Nannini-Pepe M, Kotkow K, Marsters JC, Rubin LL, de Sauvage FJ (2008) A paracrine requirement for Hedgehog signalling in cancer. *Nature* **455**: 406–410.

Supplementary Information accompanies this paper on British Journal of Cancer website (http://www.nature.com/bjc)